

Synthesis of Simultaneous Multiple-Harmonic-Patterns in Time-Modulated Linear Antenna Arrays

Sujit K. Mandal*, Gautam K. Mahanti, and Rowdra Ghatak

Abstract—In time-modulated antenna arrays (TMAAs), as a result of periodical switch-on and switch-off of the antenna elements, including operating frequency (termed as center frequency) signal, sideband signals are appeared at either sides of the center frequency in integer multiples of the modulation frequency. In this paper, it is shown that without using phase shifters, just by suitably controlling the on-time instants (OTIs) and on-time durations (OTDs) of a time-modulated linear antenna array (TMLAA) elements, simultaneously, along with a pencil beam pattern at the operating frequency, a shaped beam pattern can be obtained at both the first positive and negative harmonics of the time-modulation frequency. The important advantage of such a technique is that realization of multi-beam pattern in conventional antenna array (CAA) system generally requires complex feed network, whereas by using simple radio frequency (RF) switching circuit in the feed network of TMLAA, by virtue of the properties of harmonic radiations, synthesis of a shaped pattern at either (positive or negative) harmonic results in generating the same pattern in its opposite harmonic, and the synthesized patterns at different harmonics can be simultaneously used as independent communication channels. By employing a differential evolution (DE) based optimization method, numerical results for a 16-element TMLAA with uniform excitation show that in conjunction with a pencil beam pattern at the center frequency, a flat-top or a cosec square pattern at first positive and negative sidebands of side-lobe levels (SLL) -20 dB can be synthesized by suppressing the higher sideband level (SBL) to below -10 dB.

1. INTRODUCTION

An antenna array that is made to generate multiple radiation patterns is useful in many applications, such as surveillance and tracking in radar systems [1,2], military, satellite [3] and cellular communication [4]. In communication systems, same or different shaped multiple patterns are used adaptively to maintain a reliable wireless link in the presence of jammers or interference signal. Also to provide different requests of services in a single or multiple frequency of operation, instead of using multiple antennas. Multiple beams of antenna arrays are properly handled to serve the required services with the advantages of reduced design complexity, cost and weight of the antenna. Consequently, various methods, such as switchable [4], reconfigurable [5,6], and interleaved [2,7], have been effectively utilized to generate multiple power patterns in CAAs. Since the complexity in implementing the feed network becomes more when the element excitations for the different patterns differ both in amplitude and phase than if the element excitations differ only in phase. Therefore, reconfigurable antenna array with phase only control is a preferable technique. However, in this method, only one beam is active at any instant of time. At this juncture, interleaved array is used successfully in some radar based applications [2,7].

The time modulation (TM) technique, commenced by Shanks and Bickmore [8] in 1959, is conveniently used to realize low/ultralow SLL pattern in uniform amplitude array [9,10] or non-uniform amplitude array with low dynamic range ratio (DRR) of static amplitude [11–13]. For a

Received 18 November 2013, Accepted 9 January 2014, Scheduled 14 January 2014

* Corresponding author: Sujit Kumar Mandal (skmandal2006@yahoo.co.in).

The authors are with the Microwave and Antenna Research Laboratory, Department of Electronics and Communication Engineering, National Institute of Technology Durgapur, West Bengal, India.

specific radiation pattern in TMAA, electronically, a predetermined sequence of the relative on-time durations of the switches connected to the array elements is controlled easily, rapidly, and accurately during a fixed interval of time period. Recently, as investigated in [14], TMAA architecture with a suitable control strategy can be applied to adaptive nulling in time-varying scenarios. However, inherent sideband radiations in TMAA reduces antenna efficiency and directivity [15, 16] when the desired pattern is synthesized at the operating frequency only. Accordingly, during the last decade, a number of contributions with different time-modulation approaches based on different optimization tools have been successfully applied to realize different patterns at the operating frequency by suppressing SBLs to sufficiently low values [10–13, 17–24].

On the other hand, sideband signals can also be used in some specific applications [25–28] by controlling ‘on-off’ time instants of the antenna elements. For example, without using phase shifter, on-time sequences of each element are controlled to obtain an electronic beam steering technique at the first sideband of TMLAA [25]. Using the first sideband signal of a two-element TMLAA system, active electronic null scanning technique is experimentally verified in [26]. In the first sideband, shaped patterns (flat-top and cosec²) are synthesized in TMAAs with uniform static excitation amplitude and phase distributions [27]. In [28], a particle swarm (PS) based strategy is introduced for synthesizing broadside sum and difference, flat-top and sum pattern at center frequency and first sideband, respectively.

For a conventional antenna array with uniform inter-element spacing, phase shifter is an essential component for not only synthesizing multi-beam patterns, but also synthesizing a single shaped beam pattern as flat-top or cosec². Although in [27], flat-top and cosec² patterns are realized by controlling the sequence of OTI and OTD of the TMAA elements, the signal power radiated at the center frequency has not been taken into account. Moreover, the negative sideband pattern has not been examined after generating the patterns at the positive sideband. In this paper, we propose a novel DE-based optimization technique for synthesizing simultaneous different patterns in the multiple harmonics of time-modulated antenna arrays. The technique optimizes the sequence of OTIs and OTDs of 16-element TMLAA elements by using DE [29] to realize a low side lobe, narrow, pencil beam pattern at operating frequency and low side lobe shaped (flat-top/cosec²) beam pattern at both the first positive and negative sidebands, by suppressing the higher sideband levels.

2. THEORY

2.1. Time-Modulated Linear Antenna Array (TMLAA)

Let us assume a TMLAA of N mutually-uncoupled isotropic radiators with inter-element spacing d_0 . If t_p^i and $t_p^{on} \forall p \in [1, N]$ are the sequences of OTIs and OTDs of the array elements, as shown in Fig. 1, the switching function of the p -th element can be expressed by a periodic pulse, $U_p(t)$, such that at ν -th time-modulation period, it is given by

$$U_p(t) = \begin{cases} 1; & (vT_m + t_p^i) \leq t \leq (vT_m + t_p^i + t_p^{on}); \\ 0; & \text{elsewhere} \end{cases} \quad (1)$$

After the switching operation, the array factor expression of CAAs with uniform static excitation

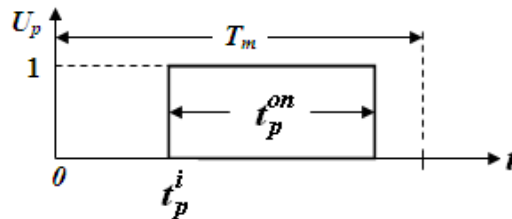


Figure 1. The on-time instant and on-time duration of the p -th element, during a time-modulation period, T_m .

amplitude and phase is modified as in (2), [25].

$$AF(\theta, t) = e^{j\omega_0 t} \sum_{p=1}^N U_p(t) e^{j\alpha_p} \quad (2)$$

where $\omega_0 = 2\pi f_0$ is the angular frequency (rad/sec) of the operating carrier signal, $\alpha_p = (p - 1)\beta d_0 \cos \theta \forall p \in [1, N]$ the linear progressive phase of p -th element, $\beta = 2\pi/\lambda$ the wave number with λ being the wave-length of the signal, and θ the observing angle measured from the array axis. Since, $U_p(t)$ is a time periodic function, (2) can be decomposed by applying Fourier series technique to obtain the power pattern at different harmonics of the modulation frequency, $\omega_m = 2\pi/T_m = 2\pi f_m$. For such an antenna array, the array factor expression at k -th harmonic is readily obtained from [25, 28] as

$$AF_k(\theta, t) = e^{j(\omega_0 + k\omega_m)t} \sum_{p=1}^N C_{p,k} e^{j\alpha_p} \quad (3)$$

where $C_{p,k}$ is the complex Fourier coefficient for the p -th element, at k -th harmonic, and is given by

$$C_{p,k} = \tau_p \frac{\sin(k\pi\tau_p)}{k\pi\tau_p} e^{-jk\pi(2\varepsilon_p + \tau_p)} \quad (4)$$

where, k belongs to a set of integer number Z ; $\{\tau_p\} = t_p^{on}/T_m$ and $\{\varepsilon_p\} = t_p^i/T_m \forall p \in [1, N]$ stand for normalized values of OTDs and OTIs, respectively. Hence, with $k = 0, 1$ and -1 , (3) and (4) can be combined to obtain the resultant array factor expression at the center (operating) frequency, first positive harmonic (sideband) and first negative harmonic (sideband) as in (5), (6) and (7), respectively.

$$AF_0(\theta, t) = e^{j\omega_0 t} \sum_{p=1}^N \tau_p e^{j\alpha_p} \quad (5)$$

$$AF_1(\theta, t) = e^{j(\omega_0 + \omega_m)t} \sum_{p=1}^N \frac{\sin(\pi\tau_p)}{\pi} e^{-j\pi(2\varepsilon_p + \tau_p)} \cdot e^{j\alpha_p} \quad (6)$$

$$AF_{-1}(\theta, t) = e^{j(\omega_0 - \omega_m)t} \sum_{p=1}^N \frac{\sin(-\pi\tau_p)}{(-\pi)} e^{j\pi(2\varepsilon_p + \tau_p)} \cdot e^{j\alpha_p} \quad (7)$$

As can be seen from (4) that with $k = 0$, Fourier coefficients of the time-modulated elements, $C_{p,0} = \tau_p \forall p \in [1, N]$, are real valued, which provide an average amplitude distribution in the array factor expression at center frequency in (5). Thus, at the center frequency, a desired broadside sum pattern can be synthesized by properly distributing the on-time sequence of the antenna elements as reported in [9, 13, 18, 22]. On the other hand, for $k \neq 0$, $C_{p,k}$ is complex, giving both excitation amplitude as $\frac{\sin(k\pi\tau_p)}{k\pi\tau_p}$ and phase as $e^{\pm jk\pi(2\varepsilon_p + \tau_p)}$, for the array factor expression at the k -th harmonic. Therefore, both the excitation amplitude and phase distribution of the required shaped patterns can be obtained at the first sideband by suitably controlling the sequence of τ_p and ε_p , as in [27]. In this paper, by using DE, the distribution of τ_p and ε_p of uniformly excited TMLAA elements are optimized to simultaneously synthesize a broadside pencil beam pattern at f_0 and shaped beam pattern at the first positive harmonic, $(f_0 + f_m)$. From (4), it can be further observed that $|C_{p,k}| = |C_{p,-k}|$ and $\angle C_{p,k} = -\angle C_{p,-k}$, i.e., the amplitude and the phase spectrum are even and odd symmetry functions of the k -th harmonic. As a result, the same power pattern as can be synthesized by using (6) should also be obtained in (7), but the pattern is flipped by 180° with respect to the maximum direction (broadside here) of the center frequency pattern. In this paper, the object is to simultaneously synthesize a pencil beam pattern at f_0 and a shaped (flat-top or cosec²) pattern at $(f_0 + f_m)$. In Section 3, it is shown that the same shaped beam pattern as synthesized at $(f_0 + f_m)$ is obtained automatically at $(f_0 - f_m)$.

2.2. Optimization Using DE

The DE algorithm is an efficient stochastic evolutionary computational method. Due to the superior search ability and faster convergence profile, it has been successfully applied to solve many antennas [10–13], electromagnetics [29] and many other optimization problems.

In order to synthesize the desired pencil beam at f_0 and shaped beam at $(f_0 + f_m)$, the on-time instants and on-time durations of the antenna elements are used as the optimization parameter vector $\chi = \{\tau_p, \varepsilon_p\}$. In the optimization process, $\{\tau_p\}$ is perturbed in the search range $[0, 1]$ whereas for $\{\varepsilon_p\}$, the search range is defined as $\{1 - \tau_p\}$. Thus unlike [28], $(\tau_p + \varepsilon_p)$ is always ≤ 1 , and complex Fourier coefficients is obtained only by using (4). To obtain a good result in DE, the control parameters are set as — number of population (N_{POP}) = $5D$ (D being the dimension of the problem), mutation constant (F) = 0.5 and crossover constant (η_c) = 0.9. The cost function for the DE is defined as

$$\psi(\chi^g) = \sum_{k=0}^2 \sum_{\delta_{k,i} \in \{\mathfrak{R}_k\}} W_{\delta_{k,i}} \cdot H\left(\left|\delta_{k,i}^d\right| - \left|\delta_{k,i}(\chi^g)\right|\right) \cdot \left|\delta_{k,i}^d - \delta_{k,i}(\chi^g)\right|. \quad (8)$$

where $\delta_{k,i}$ represents the i -th design parameters of the k -th harmonic pattern with $\delta_{k,i}^d$ being their corresponding desired values; \mathfrak{R}_k is the set of design parameters for k -th harmonic pattern, such as for $k = 0$, $\mathfrak{R}_0 = \{\text{SLL}_0, \text{FNBW}\}$, for $k = 1$, $\mathfrak{R}_1 = \{\text{SLL}_1, \text{Ripple}, \text{SBL}_1\}$, and for $k = 2$, $\mathfrak{R}_2 = \{\text{SBL}_2\}$. Hence, $\delta_{0,1}$ represents the SLL ($\delta_{0,1} \leftarrow \text{SLL}_0$), and $\delta_{0,2}$ is the first null beam width ($\delta_{0,2} \leftarrow \text{FNBW}$) of the pencil beam pattern at f_0 . Similarly, $\delta_{1,1}$, $\delta_{1,2}$ and $\delta_{1,3}$ denote SLL₁ ($\delta_{1,1} \leftarrow \text{SLL}_1$), ripple level ($\delta_{1,2} \leftarrow \text{Ripple}$) and SBL ($\delta_{1,3} \leftarrow \text{SBL}_1$) for the shaped beam (flat-top/cosec²) pattern at $(f_0 + f_m)$, and $\delta_{2,1}$ is the SBL ($\delta_{2,1} \leftarrow \text{SBL}_2$) of the second sideband, respectively. ‘ $W_{\delta_{k,i}}$ ’ is the weighting factors of the corresponding terms. $H(\cdot)$ is the Heaviside step function and χ^g the optimization parameter vector at the generation index ‘ g ’ of the optimization algorithm, DE. During minimization of the cost function Ψ , the design parameters, SLL and SBL are measured in dB and FNBW in deg.

3. NUMERICAL RESULTS

A TMLAA with $N = 16$ and $d_0 = 0.5\lambda$ is considered. In the first example, a broadside pencil beam and flat-top beam of flat beam width 30° ($-0.26 \leq u \leq 0.26$) and sharp transition of 8° ($\pm 0.26 < u \leq \pm 0.4$)

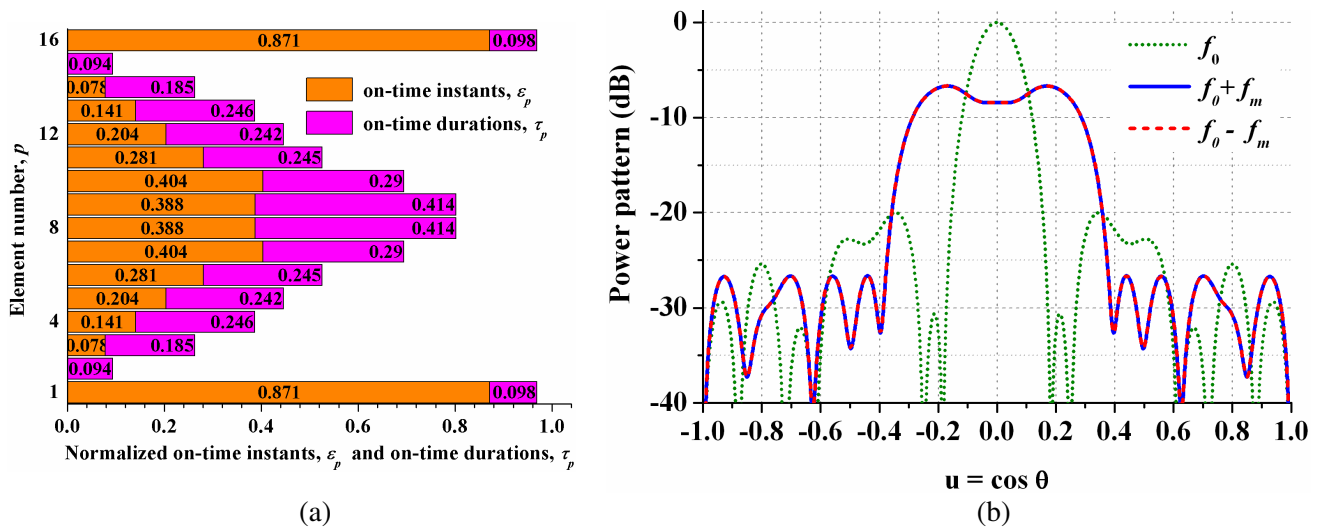


Figure 2. Generation of simultaneous pencil and flat-top pattern at f_0 and $f_0 \pm f_m$. (a) On-time instants, ‘ ε_p ’ and on-time durations, ‘ τ_p ’ of the array elements. (b) Relative power pattern at f_0 and $f_0 \pm f_m$.

are selected as the target patterns at f_0 and $(f_0 + f_m)$, respectively. Due to symmetry in the shape of the flat-top pattern, symmetrical distributions of τ_p and ε_p of the array elements are considered. As a result, the dimension of the synthesis problem is reduced to 16 unknown variables. With $k = 0, 1$ and 2, the set of design parameters in (8) are chosen as $\mathfrak{R}_0 = \{-20, 21\}$, $\mathfrak{R}_1 = \{-20, 1.5, -6.5\}$ and $\mathfrak{R}_2 = \{-10\}$, respectively. In the sets, the numerical values corresponding to SLL, SBL and ripple level are in dB and for FNBW in degree. By setting all $W_{\delta_k} = 1$, DE takes 700 iterations to determine the distribution of τ_p and ε_p as shown in Fig. 2(a). The corresponding relative radiation patterns at f_0 and $(f_0 \pm f_m)$ are shown in Fig. 2(b). It can be observed in Fig. 2(a) that due to symmetry in the shape of the broadside flat-top pattern, 180° rotation of the pattern at $(f_0 - f_m)$ around the broadside direction gives the same pattern as it is synthesized at $(f_0 + f_m)$. The sets of the design parameters as obtained in Fig. 2(b), are $\mathfrak{R}_0 = \{-20, 21.2\}$, $\mathfrak{R}_1 = \{-19.96, 1.76, -6.67\}$ and $\mathfrak{R}_2 = \{-11.48\}$, respectively. Since in [28] the desired flat-top pattern is synthesized at f_0 , the method reported in [28] needs phase shifters to provide the necessary excitation phase distribution of the antenna elements.

In the second example, the target pattern at $(f_0 + f_m)$ is a cosec² pattern in the range $0 \leq u \leq 0.5$.

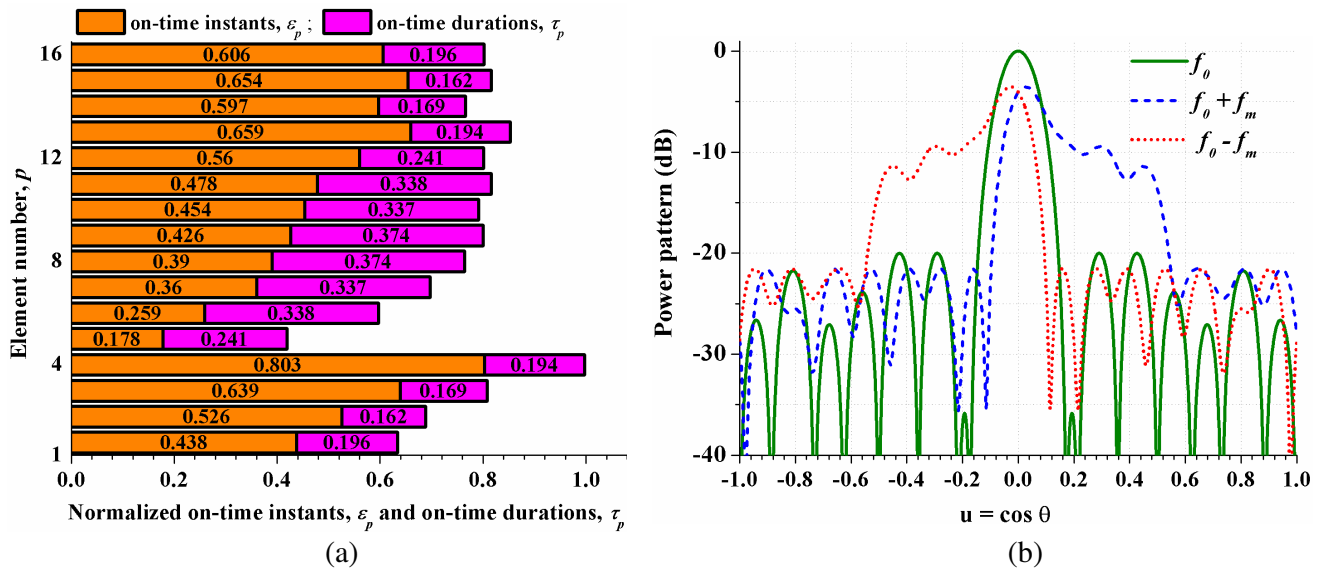


Figure 3. Generation of simultaneous pencil beam at f_0 and cosec² pattern at $f_0 \pm f_m$. (a) On-time instants, ‘ ε_p ’ and on-time durations, ‘ τ_p ’ of the array elements. (b) Relative power pattern at f_0 and $f_0 \pm f_m$.

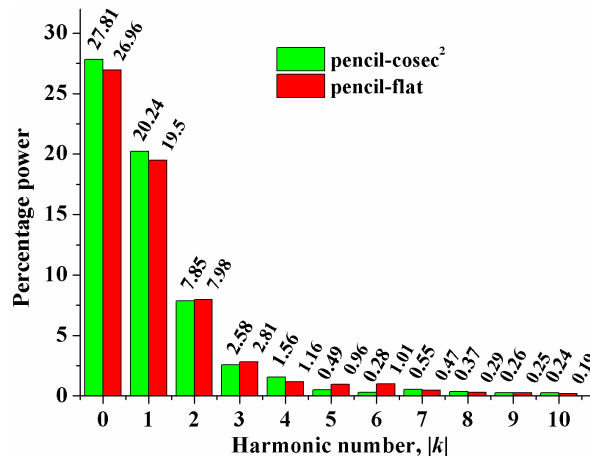


Figure 4. The percentage power distribution at different harmonics when OTIs and OTDs as shown in Figs. 2(a) and 3(a) are used in a 16 element TMLAA with uniform amplitude and phase.

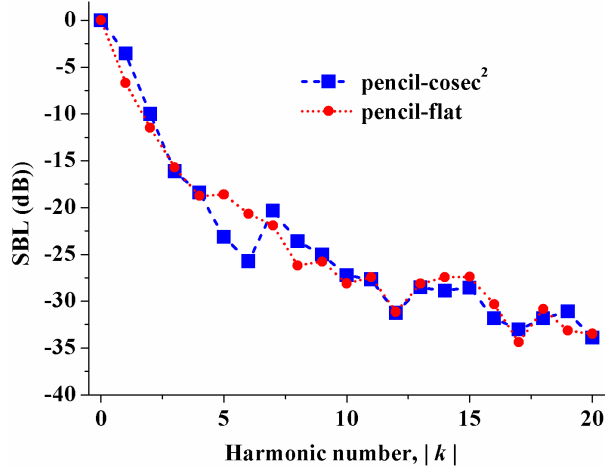


Figure 5. The sideband level of first 20 sidebands for the power pattern shown in Figs. 2(b) and 3(b).

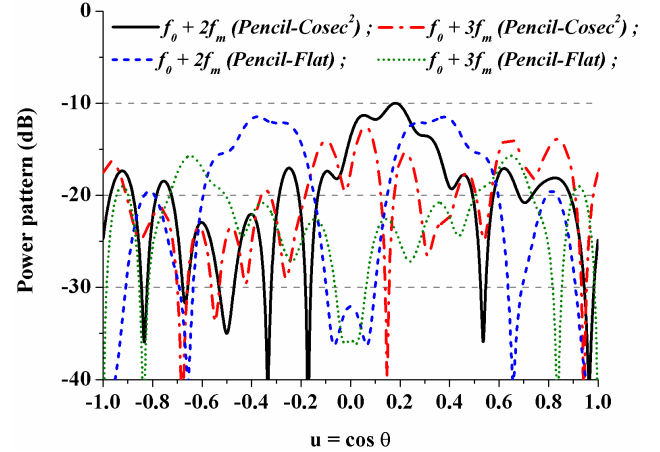


Figure 6. For a 16 element uniform amplitude TMLAA, the relative power pattern at second sideband, $f_0 + 2f_m$ and third sideband, $f_0 + 3f_m$ when OTIs and OTDs of Figs. 2(a) and 3(a) are used.

The desired design parameters sets are taken as $\mathfrak{R}_0 = \{-20, 20\}$, $\mathfrak{R}_1 = \{-19, 1.5, -3.5\}$ and $\mathfrak{R}_2 = \{-10\}$, respectively. As the cosec² beam is asymmetrical in shape, only symmetrical distribution of τ_p is considered. Hence the dimension of the problem becomes 24. Empirically, all the weighting factors are made equal to 1 except one that is corresponding to the ripple, which is made equal to 3. Fig. 3(a) shows the DE optimized τ_p and ε_p obtained after 1000 iterations. Fig. 3(b) shows the relative power pattern at f_0 , $(f_0 + f_m)$ and $(f_0 - f_m)$. It can be seen from Fig. 3(b) that the pattern at $(f_0 - f_m)$ is the same as that in $(f_0 + f_m)$ but flipped around the broadside direction. In the synthesized patterns in Fig. 3(b), the obtained design parameters are $\mathfrak{R}_0 = \{-20, 19.96\}$, $\mathfrak{R}_1 = \{-18, 1.14, -3.53\}$ and $\mathfrak{R}_2 = \{-10\}$. Thus, DE synthesizes the patterns close to their required design parameter values. Fig. 4 shows the percentage of total power radiated at different sidebands k , with $k \in [0, 10]$. As can be seen, most of the total power is radiated at f_0 and $(f_0 \pm f_m)$ to generate the desired patterns, and at higher harmonics, the amount of radiated power tends to zero rapidly. Fig. 5 shows the sideband levels of the synthesized patterns at different harmonic numbers $k \in [0, 20]$. To observe the nature of the power patterns at higher harmonics, the relative power pattern for $k = 2$ and 3 are also plotted in Fig. 6. Although in Figs. 5 and 6, SBLs at second sideband are only 4.81 and 6.47 dB less than those obtained in the first sideband for the above two examples, respectively, it has been observed that by setting the desired value of SBL at the second sideband to -20 dB and keeping all other design parameters of (8) the same as used in the respective examples, almost same patterns with newly set desired value of SBL at the 2nd sideband are obtained. However, the power level at the 1st sideband is reduced by 1–2 dB, and FNBW of the pencil beam pattern is increased by 0.5–2 deg from its previous values.

4. CONCLUSION

A novel technique, for synthesizing simultaneous multiple patterns at harmonics of uniformly excited TMLAA, is presented. Only by optimizing the on-time instants and on-time durations of the antenna elements using DE, a low side-lobe broadside pencil-beam pattern at center frequency and a shaped (flat-top and cosec²) beam pattern at the first positive sideband are synthesized. As per the theory of time modulation, the same pattern as synthesized in the first positive sideband is realized at the first negative sideband. Thus, three patterns are simultaneously obtained at three different harmonics. The proposed method is useful as it does not require any phase shifters which have high insertion loss up to 13 dB or more. In addition, the high cost of phase shifters greatly increases the total cost of the antenna array system.

REFERENCES

1. Johnson, R. C., and H. Jasik, *Antenna Applications Reference Guide*, The McGraw-Hill Engineering Guide Series, New York, 1984.
2. Lager, I. E., C. Trampuz, M. Simeoni, and L. P. Ligthart, "Interleaved array antennas for FMCW radar applications," *IEEE Transaction on Antennas and Propagation*, Vol. 57, No. 8, 2486–2490, Aug. 2009.
3. Sudhakar R. K., G. A. Morin, M. Q. Tang, and S. Richard, "Development of a 45 GHz multiple-beam antenna for military satellite communications," *IEEE Transaction on Antennas and Propagation*, Vol. 45, No. 10, 1036–1047, 1995.
4. Barba, M., J. E. Page, J. A. Encinar, and J. R. Montejo-Garai, "A switchable multiple beam antenna for GSM-UMTS base stations in planar technology," *IEEE Transaction on Antennas and Propagation*, Vol. 54, No. 11, 3087–3094, Nov. 2006.
5. Bucci, O. M., G. Mazzarella, and G. Panariello, "Reconfigurable arrays by phase-only control," *IEEE Transaction on Antennas and Propagation*, Vol. 39, No. 7, 919–925, 1991.
6. Durr, M., A. Trastoy, and F. Ares, "Multiple-pattern linear antenna arrays with single prefixed amplitude distributions: Modified Woodward-Lawson synthesis," *Electron. Lett.*, Vol. 36, No. 16, 1345–1346, 2000.
7. Oliveri, G. and A. Massa, "Fully-interleaved linear arrays with predictable sidelobes based on almost difference sets," *IET Radar Sonar Navigat.*, Vol. 4, No. 5, 649–661, 2010.
8. Shanks, H. E. and R. W. Bickmore, "Four dimensional electromagnetic radiators," *Canad. J. Phys.*, Vol. 37, No. 3, 263–275, 1959.
9. Kummer, W. H., A. T. Villeneuve, T. S. Fong, and F. G. Terrio, "Ultra-low side-lobes from time-modulated arrays," *IEEE Transaction on Antennas and Propagation*, Vol. 1, No. 6, 633–639, 1963.
10. Zhu, Q., S. Yang, L. Zheng, and Z. Nie, "Design of a low side lobe time modulated linear array with uniform amplitude and subsectional optimized time steps," *IEEE Transaction on Antennas and Propagation*, Vol. 60, No. 9, 4436–4439, Sep. 2012.
11. Yang, S., Y. B. Gan, and A. Qing, "Sideband suppression in time-modulated linear arrays by the differential evolution algorithm," *IEEE Antennas Wireless Propag. Lett.*, Vol. 1, 173–175, 2002.
12. Yang, S., Y. B. Gan, and P. K. Tan, "A new technique for power-pattern synthesis in time-modulated linear arrays," *IEEE Antennas Wireless Propag. Lett.*, Vol. 2, 285–287, 2003.
13. Mandal, S. K., G. K. Mahanti, and R. Ghatak, "A single objective approach for suppressing sideband radiations of ultra-low side lobe patterns in time-modulated antenna arrays," *Journal of Electromagnetic Waves and Applications*, Vol. 27, No. 14, 1767–1775, 2013.
14. Rocca, P., L. Poli, G. Oliveri, and A. Massa, "Adaptive nulling in time-varying scenarios through time-modulated linear arrays," *IEEE Antennas Wireless Propag. Lett.*, Vol. 11, 101–104, 2012.
15. Bregains, J. C., J. Fondevila-Gomez, G. Franceschetti, and F. Ares, "Signal radiation and power losses of time-modulated arrays," *IEEE Transaction on Antennas and Propagation*, Vol. 56, No. 6, 1799–1804, 2008.
16. Yang, S., Y. B. Gan, and P. K. Tan, "Evaluation of directivity and gain for time-modulated linear antenna arrays," *Microw. Opt. Technol. Lett.*, Vol. 42, No. 2, 167–171, 2004.
17. Fondevila, J., J. C. Brégains, F. Ares, and E. Moreno, "Application of time-modulation in the synthesis of sum and difference patterns by using linear arrays," *Microw. Opt. Technol. Lett.*, Vol. 48, 829–832, 2006.
18. Yang, S., Y. B. Gan, A. Qing, and P. K. Tan, "Design of uniform amplitude time modulated linear array with optimized time sequences," *IEEE Transaction on Antennas and Propagation*, Vol. 53, No. 7, 2337–2339, 2005.
19. Poli, L., P. Rocca, L. Manica, and A. Massa, "Pattern synthesis in time-modulated linear arrays through pulse shifting," *IET Microw. Antennas Propag.*, Vol. 4, No. 9, 1157–1164, 2010.
20. Rocca, P., L. Poli, G. Oliveri, and A. Massa, "Synthesis of sub-arrayed time modulated linear arrays through a multi-stage approach," *IEEE Transaction on Antennas and Propagation*, Vol. 59,

- No. 9, 3246–3254, Sep. 2011.
21. Rocca, P., L. Manica, L. Poli, and A. Massa, “Synthesis of compromise sum-difference arrays through time-modulation,” *IET Radar, Sonar & Navigation*, Vol. 3, No. 6, 630–637, 2009.
 22. Poli, L., P. Rocca, L. Manica, and A. Massa, “Handling sideband radiations in time-modulated arrays through particle swarm optimization,” *IEEE Transaction on Antennas and Propagation*, Vol. 58, No. 4, 1408–1411, Apr. 2010.
 23. Poli, L., P. Rocca, L. Manica, and A. Massa, “Time modulated planar arrays — Analysis and optimization of the sideband radiations,” *IET Microwaves, Antennas & Propagation*, Vol. 4, No. 9, 1165–1171, 2010.
 24. Bekele, E. T., L. Poli, M. D’Urso, P. Rocca, and A. Massa, “Pulse-shaping strategy for time modulated arrays — Analysis and design,” *IEEE Transaction on Antennas and Propagation*, Vol. 61, No. 7, 3525–3537, Jul. 2013.
 25. Li, G., S. Yang, Y. Chen, and Z.-P. Nie, “A novel electronic beam steering technique in time modulated antenna arrays,” *Progress In Electromagnetics Research*, Vol. 97, 391–405, 2009.
 26. Tennant, A., “Experimental two-element time-modulated direction finding array,” *IEEE Transaction on Antennas and Propagation*, Vol. 58, No. 3, 986–988, Mar. 2010.
 27. Gang, L., S. Yang, M. Huang, and Z. Nie, “Shaped patterns synthesis in time-modulated antenna arrays with static uniform amplitude and phase excitations,” *Front. Electr. Electron. Eng. China*, Vol. 5, No. 2, 179–184, Jun. 2010.
 28. Poli, L., P. Rocca, G. Oliveri, and A. Massa, “Harmonic beam forming in time modulated linear arrays,” *IEEE Transaction on Antennas and Propagation*, Vol. 59, No. 7, 2538–2545, 2011.
 29. Rocca, P., G. Oliveri, and A. Massa, “Differential evolution as applied to electromagnetics,” *IEEE Antennas Propag. Mag.*, Vol. 53, No. 1, 38–49, Feb. 2011.